Journal of Alloys and Compounds 500 (2010) 113–116

Contents lists available at ScienceDirect

Journal of Alloys and Compounds

journal homepage: www.elsevier.com/locate/jallcom

Influence of annealing temperature and doping rate on the magnetic properties of Zr–Mn substituted Sr-hexaferrite nanoparticles

Muhammad Javed Iqbal[a], Muhammad Naeem Ashiq[b], Pablo Hernández-Gómez[c,*], José María Muñoz Muñoz[c], Carlos Torres Cabrera[c]

[a] Department of Chemistry, Quaid-i-Azam University, Islamabad 45320, Pakistan
[b] Department of Chemistry, Bahauddin Zakariya University, Multan, Pakistan
[c] Dpt. Electricidad y Electrónica, University of Valladolid, 47071 Valladolid, Spain

ARTICLE INFO

Article history:
Received 27 October 2009
Received in revised form 23 March 2010
Accepted 31 March 2010
Available online 7 April 2010

PACS:
75.50 Gg
75.50Tt
75.60Ej

Keywords:
Magnetically ordered materials
Oxide materials
Magnetisation
Magnetic measurements

ABSTRACT

A series of M-type strontium hexaferrite samples having nominal composition $SrZr_xMn_xFe_{12-2x}O_{19}$ (where $x = 0.0–0.8$) has been synthesized by the co-precipitation method. All the samples synthesized were of single magnetoplumbite phase. The particle size was found to be in the 40–65 nm range for the samples annealed at 1193 K while the samples annealed at 1443 K were in the 100–200 nm range. The saturation magnetization increase with temperature and reached maxima for the samples annealed at 1393 K and then start to decrease while the coercivity decreases regularly with temperature. The decrease in coercivity is due to the increase in the particle size of the sample with temperature. The saturation magnetization increase for the samples doped with Zr–Mn up to $x = 0.4$ doping rate and higher substitution lead to decrease in saturation magnetization. The coercivity decrease with the increase in Zr–Mn substitution. The behavior of saturation magnetization has been explained on the basis of occupation of the substituted cations at different iron sites. The increase in saturation magnetization and decrease in coercivity suggest that the synthesized materials can be used for the application of recording media.

1. Introduction

Recently, M-type strontium and barium hexagonal ferrites have attracted a lot of attention because of their excellent magnetic properties and potential applications in various fields. Their properties of large magnetocrystalline anisotropy, high saturation magnetization, coercivity and corrosion resistivity results in their usage as plastic magnetic, recording media, permanent magnetic and as components in microwave and high frequency devices [1–12]. The M-type hexagonal unit cell contains two formula units and is made of 10 oxygen layers. It can be described as RSR*S*, where *R* is a three oxygen layer block comprising of $(Ba^{2+}$ or $Sr^{2+}Fe_6{}^{3+}O_{11})^{2-}$, while *S* block contains $(Fe_6{}^{3+}O_8)^{2+}$ and the *R** and *S** indicate the blocks obtained by rotating *S* and *R* through 180° around the *c*-axis [13]. The magnetic properties of the hexagonal ferrites are strongly dependent upon the synthesis conditions and the site preference of the substituted cations among the five different Fe^{3+} sublattices namely, tetrahedral ($4f_1$), trigonal bipyramidal (2b) and octahedral (12k, 2a and $4f_2$) of hexagonal structure [14].

Single domain particles of Ti–Co and Ti–Ni substituted M-type hexaferrite posses attractive properties for the recording media applications [15]. Such substitutions at iron site are effective in reducing the coercivity and magnetocrystalline anisotropy but require higher annealing temperature for the formation of single phase. It has also been reported that when synthesizing Ti–Ni substituted hexaferrites, it is difficult to avoid the formation of nickel ferrite [16]. Although the coercivity decrease by the substitution of Ti–Ni but at the same time the saturation magnetization of the materials decrease which limit their applications in the high density recording media. Zr^{4+} that is isoelectronic with Ti^{4+} has been selected for the present study along with Mn^{2+} to maintain overall electroneutrality. The aim of this work is to decrease the coercivity and to increase the saturation magnetization simultaneously. This paper presents the effect of annealing temperature and substitution rate of Zr–Mn on the magnetic properties of strontium hexaferrite nanoparticles synthesized by co-precipitation method.

2. Experimental

Chemicals used in the synthesis of samples were $Fe(NO_3)_3{\cdot}9H_2O$ (Panreac Quimica SA, 98%), $Sr(NO_3)_2$ (Fluka, ≥99%), $ZrOCl_2{\cdot}4H_2O$ (BDH, 96%), $Mn(CH_3COO)_2{\cdot}4H_2O$ (Merck, 98%) and NaOH (Fluka, ≥97%). The strontium hexaferrite samples substi-

* Corresponding author. Tel.: +34 983423225.
E-mail address: pabloher@ee.uva.es (P. Hernández-Gómez).

0925-8388/$ – see front matter © 2010 Elsevier B.V. All rights reserved.
doi:10.1016/j.jallcom.2010.03.228

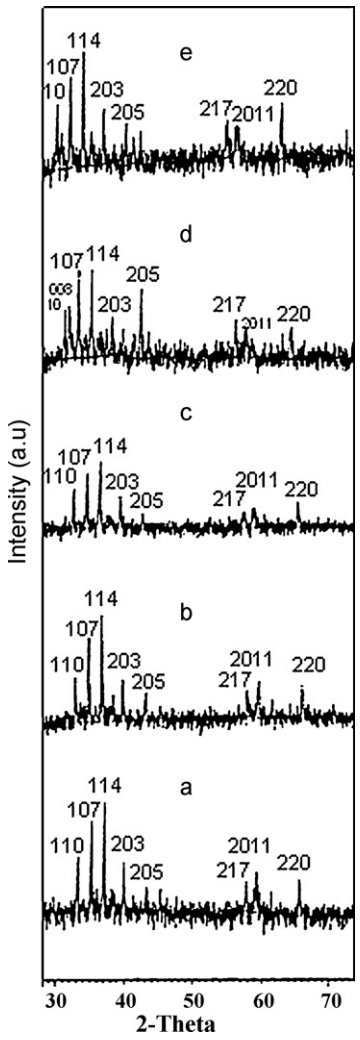

Fig. 1. The indexed XRD patterns of Sr-hexaferrite doped with Zr_xMn_x (a) $x = 0.0$, (b) $x = 0.2$, (c) $x = 0.4$, (d) $x = 0.6$ and (e) $x = 0.8$.

tuted with Zr–Mn and having nominal composition $SrZr_xMn_xFe_{12-2x}O_{19}$ (where $x = 0.0$–0.8) were prepared by a chemical co-precipitation method [10] keeping the molar ratio (Fe/Sr = 11). The theoretical ratio of Fe/Sr = 12.0 as in chemical formula is obtained when the Fe/Sr ratio is kept 11.0. This is due to the higher solubility of Fe than that of Sr and it is necessary to keep the concentration of strontium slightly higher to obtain the pure hexagonal phase. The 2 M solution of NaOH was used as precipitating agent. The detail of experiment can be found in Ref. [17].

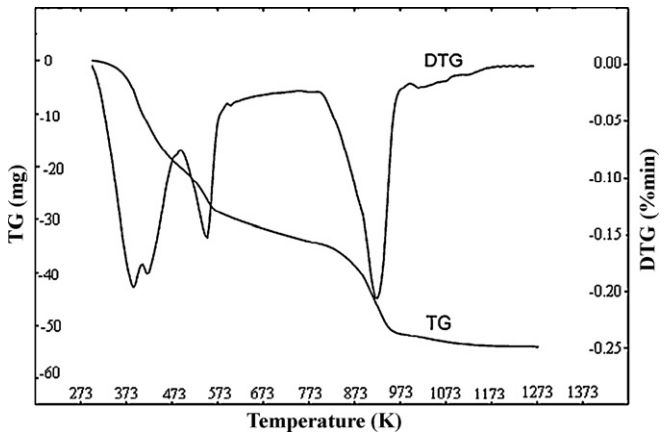

Fig. 3. TG/DTG curve of $SrZr_{0.4}Mn_{0.4}Fe_{11.2}O_{19}$.

The precipitates were annealed at temperature of 1193 K for 1 h to obtain the single phase. Transmission electron microscopy (TEM) analysis is carried out using JEOL JEM-1200EX. The TG/DTG analysis of $SrZr_{0.4}Mn_{0.4}Fe_{11.2}O_{19}$ was done by a thermobalance (Setaram TGA-92) operating at a heating rate of 5 K/min from room temperature to 1273 K. The hysteresis loops of the samples are measured for all the samples annealed at different temperature 1193, 1293, 1393 and 1443 K for 1 h using system containing a standard AC induction method [18], in which the magnetic field H and the magnetic induction B are both measured through two coils placed near the sample and saturation magnetization, remanence and coercivity are calculated. The Curie temperature was determined from temperature dependence of ac magnetic susceptibility data. The ac magnetic susceptibility was measured by primary and secondary coil set up operating at frequency of 273 Hz [19].

3. Results and discussion

All the samples have the single magnetoplumbite phase which was already characterized by XRD (Fig. 1) and FTIR analysis [19]. The TEM measurements (Fig. 2) were used to evaluate the particle size of the synthesized samples estimated with the help of the Scherrer formula using XRD pattern. The particle was found to have flat platelet shape (Fig. 2b), with diameters in the largest dimension in the range of 40–65 nm for the sample annealed at 1193 K, that increases to 100–200 nm for the samples annealed at 1443 K. Fig. 3 shows the effect of heating on the weight loss of an unannealed sample of Zr–Mn ($x = 0.4$) substituted strontium hexaferrite synthesized by co-precipitation method by TG/DTG analysis. The thermogravimetric curve shows a peak at 373 K which is due to loss of water from the sample. The other peak appeared at 573 and 900 K indicating the formation of oxides from hydroxides, monohexaferrite and the formation of hexagonal phase, respectively. The following reaction scheme may be possible:

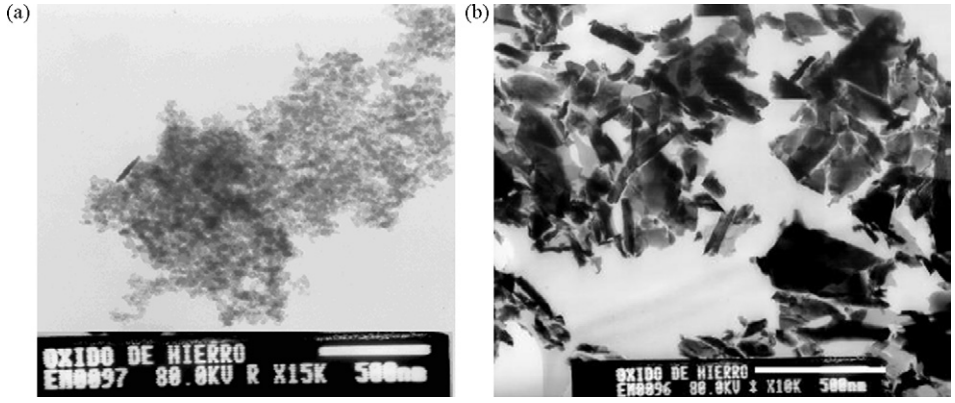

Fig. 2. TEM micrographs for $SrZr_{0.4}Mn_{0.4}Fe_{11.2}O_{19}$ (a) = at 1193 K and (b) = 1443 K.

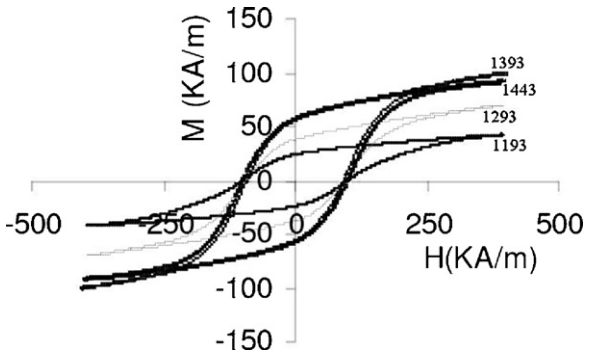

Fig. 4. Hysteresis loops of $SrZr_{0.6}Mn_{0.6}Fe_{10.8}O_{19}$.

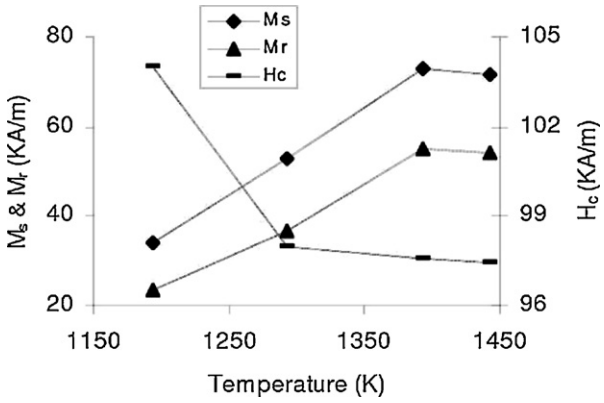

Fig. 5. Effect of annealing temperature on the saturation magnetization (M_s), remanence (M_r) and coercivity (H_c) of $SrZr_{0.6}Mn_{0.6}Fe_{10.8}O_{19}$.

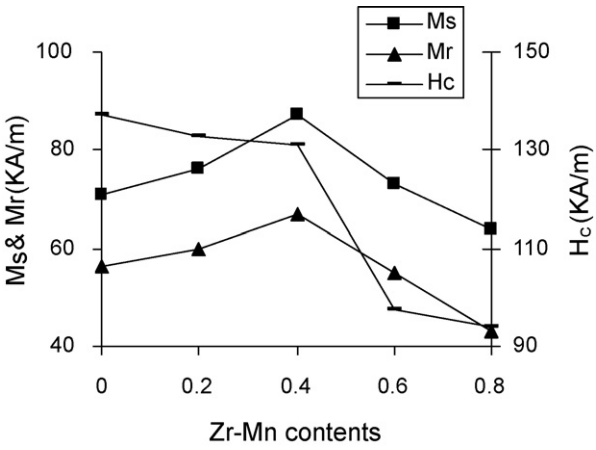

Fig. 6. Effect of Zr–Mn substitution on the saturation magnetization (M_s), remanence (M_r) and coercivity (H_c) of $SrZr_xMn_xFe_{12-2x}O_{19}$.

$$Sr(NO_3)_2\ (aq) + 11.2Fe(NO_3)_3\ (aq) + 0.4Mn(CH_3COO)_2\ (aq) + 0.4ZrOCl_2\ (aq) + 2M\ NaOH\ (aq)$$

$$\downarrow \text{pH} = 12.5\text{-}13.0$$

$$wSr.xFe.yZr.zMn(OH)_{2w+3x+4y+2z}.nH_2O + NaNO_3 + NaCl + CH_3COONa$$

$$\downarrow 573K$$

$$wSr.xFe.yZr.zMn(O)_{2w+3x+4y+2z}$$

$$\downarrow 900\text{-}1100K$$

$$SrZr_{0.4}Mn_{0.4}Fe_{11.2}O_{19}$$

According to this schema we have annealed the samples at different temperatures above 900 K to evaluate the effect of annealing temperature and find the optimal one for the different magnetic properties. Fig. 4 shows the hysteresis loops for $SrZr_{0.6}Mn_{0.6}Fe_{10.8}O_{19}$ at different temperatures and various magnetic properties such as saturation magnetization, remanence and coercivity were calculated. The shape and the width of the hysteresis loop depend on factors such as chemical composition, cation distribution, porosity, grain size, etc. The loops are wide having large value of coercivity indicating that the synthesized materials are belonging to class of hard ferrite. Fig. 5 shows the effect of annealing temperature on the saturation magnetization (M_s), remanence (M_r) and coercivity (H_c) of $SrZr_{0.6}Mn_{0.6}Fe_{10.8}O_{19}$. The maximum values of saturation magnetization and remanence were obtained when annealing at 1393 K and higher temperatures. This saturation magnetization increase with annealing temperature can be understood taking into account that the higher the annealing temperature, the higher the average particle size, so that the amount of superparamagnetic particles in the sample decreases, thus allowing a increase in the overall magnetization. It means that Zr–Mn substituted hexaferrites required higher temperature to achieve this maximum value regarding the pure strontium hexaferrite, as the pure sample acquire the maximum saturation magnetization when annealing at 1293 K. The coercivity of the samples decreased with increasing temperature. As the temperature increases the particle size also increase which results in the formation of multodomains which is responsible for the reduction in the values of coercivity. The results similar to above mentioned have also been reported earlier, i.e., the values of both the 'H_c' and 'M_s' increase up to a specific annealing temperature and then decrease [20,21]. In the earlier reported strontium hexaferrite system, the maximum values of saturation magnetization and coercivity were obtained at 1373 K but in the present study the maximum values are obtained at lower temperature of 1293 K.

The effect of substitution of Zr–Mn on the saturation magnetization, remanence and the coercivity which were annealed at 1393 K is shown in Fig. 6. It is clear from the figure that the saturation magnetization increase with the Zr–Mn substitution, reaching to maxima at $x = 0.4$ and then decrease with increasing the doping rate. On the other hand, the coercivity of the samples decreases continuously with the Zr–Mn content. It has been reported that Mn^{2+} ions occupy 12k and 2a sites [22] while the Zr^{4+} ions replace the iron ions from 2b at low substitution ($x = 0.1$) and at $4f_1$ for higher substitution ($x > 0.1$) [23]. The electrons in 12k, 2a and 2b sites have spin up direction while in $4f_1$ and $4f_2$ are spin down. The replacement of Fe^{3+} by Mn^{2+} ions mainly do not affect on the saturation magnetization because both (Fe^{3+} and Mn^{2+}) have five unpaired electrons in their outermost shell and both have the magnetic moment of $5\mu_B$. The improvement in the saturation magnetization ($x = 0.0$–0.4) is due to the replacement of Fe^{3+} by Zr^{4+} ion at $4f_1$ site. When a nonmagnetic Zr^{4+} cation replace the Fe^{3+} at $4f_1$ sites (having spin

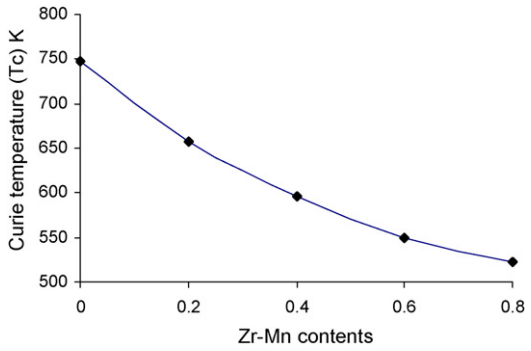

Fig. 7. Effect of Zr–Mn concentration on Curie temperature (T_c) of the synthesized samples.

down) then the total number of electrons in upward spin has been increased which cause to increase the saturation magnetization.

However, when x continues to increase above $x = 0.4$, the amount of Fe^{3+} replaced by nonmagnetic Zr^{4+} ions increase too much which lead to weakening of all the exchange interactions between $4f_1$-12k and $4f_1$-2a, as a result, the saturation magnetization decreased. The coercivity again decreased with the increase in Zr–Mn content due to decrease in magnetocrystalline anisotropy because occupation of Mn ions at 12k and 2a sites have negative influence on the anisotropy [23]. At low doping level the Zr^{4+} replace the Fe^{3+} at the trigonal bipyramidal (2b) site which also has strong influence on the magnetocrystalline anisotropy and result in the reduction of coecivity.

There are few examples in which the saturation magnetization increased and at the same time the coercivity decreased with substitutions in M-type hexaferrites. The recording media requires high enough coercivity above 47.8 kA m^{-1} and saturation magnetization as high as possible [24]. The coercivity decreased drastically from 137 kA m^{-1} to 94 kA m^{-1} for Zr–Mn substitution. On the basis of this the synthesized materials can be used for the application of recording media. The saturation magnetization increased from 71 to 87 KA/m for Zr–Mn substitutions which is also a strong evidence for their application in the recording media.

The effect of substitution on the Curie temperature is also shown in Fig. 7. It is clear from it that the Curie temperature decreases with the increase in Zr–Mn concentration. The decrease in T_c is due to the weakening of interactions between 12k-$4f_1$ and 2a-$4f_1$ due to occupation of nonmagnetic ions at $4f_1$ site.

4. Conclusion

A simple and economic method has been applied for the synthesis of Zr–Mn substituted strontium hexaferrite nanomaterials. The particle size was found in the range of 40–65 nm and was increased with the annealing temperature. These particle sizes are enough to obtain a suitable signal-to-noise ratio in the high density recoding media. The saturation magnetization increased from 71 to 87 kA/m while the coercivity decreases from 137 to 94 kA/m with the substitution of Zr–Mn content. The increase in saturation magnetization and at the same time the decrease in coercivity strongly suggest that the synthesize materials are suitable for applications in the high density recording media.

Acknowledgements

This work has been partially supported by Junta de Castilla y León research project, and IRSIP project of Pakistan Higher Education Commission (HEC). The author (MNA) is also thankful to Bahauddin Zakariya University, Multan for partially financial support.

References

[1] S.E. Jacobo, L. Civale, M.A. Blesa, J. Magn. Magn. Mater. 260 (2003) 37.
[2] N. Yang, H. Jia, J. Pang J. Alloys Compd. 438 (2007) 262.
[3] Z. Jin, W. Tang, J. Zhang, H. Lin, Y. Du, J. Magn. Magn. Mater. 182 (1998) 231.
[4] J. Qiu, M. Gu, H. Shen, J. Magn. Magn. Mater. 295 (2005) 263.
[5] B.T. Shrink, W.R. Buessem, J. Appl. Phys. 40 (1969) 1294.
[6] H. Fahlenbrach, H. Heister, Arch. Eisenhuttenwes. 29 (1953) 523.
[7] F. Haberey, A. Kockel, IEEE Trans. Magn. 12 (1976) 983.
[8] C. Surig, K.A. Hempel, D. Donnenberg, IEEE Trans. Magn. 30 (1994) 4092.
[9] J. Ding, W.F. Miao, P.G. McCormick, R. Street, J. Alloys Compd. 281 (1998) 32.
[10] A. Calleja, E. Tijero, B. Martinez, S. Pinol, F. Sandiumenge, X. Obradors, J. Magn. Magn. Mater. 196–197 (1999) 293.
[11] J.F. Hochepied, M.P. Pileni, J. Appl. Phys. 87 (2000) 2472.
[12] J.J. Went, G.W. Rathenau, E.W. Gorter, G.W. Oosterhout, Philips Tech. Rev. 13 (1952) 194.
[13] B. Kaur, M. Bhat, F. Licii, R. Kumar, S.D. Kulkarni, P.A. Joy, K.K. Bamzai, P.N. Kotru, J. Magn. Magn. Mater. 305 (2006) 392.
[14] M.J. Iqbal, M.N. Ashiq, P.H. Gomez, J.M. Munoz, J. Magn. Magn. Mater. 320 (2008) 881.
[15] N. Sugita, M. Maekawa, Y. Ohta, K. Okinaka, N. Nagai, IEEE Trans. Magn. 31 (1995) 2854.
[16] G. Turilli, F. Licci, A. Paoluzi, T. Besagni, IEEE Trans. Magn. 24 (1988) 2146.
[17] M.J. Iqbal, M.N. Ashiq, Chem. Eng. J. 136 (2008) 383.
[18] M.J. Iqbal, M.N. Ashiq, P.H. Gomez, J.M. Munoz, Scripta Mater. 57 (2007) 1093.
[19] M.J. Iqbal, M.N. Ashiq, Scripta Mater. 56 (2007) 145.
[20] J.F. Wang, C.B. Ponton, R. Grossinger, I.R. Harris, J. Alloys Compd. 369 (2004) 170.
[21] J.F. Wang, C.B. Ponton, I.R. Harris, J. Alloys Compd. 403 (2005) 104.
[22] H. Fu, H.R. Zhai, Y.C. Zhang, B.X. Gu, Y.J. Li, J. Magn. Magn. Mater. 54–57 (1986) 905.
[23] M.V. Rane, D. Bahadur, A.K. Nigam, C.M. Srivastava, J. Magn. Magn. Mater. 192 (1999) 288.
[24] Y. Li, R. Liu, Z. Zhang, C. Xiong, Mater. Chem. Phys. 64 (2000) 256.